On ion recycling and electron heating in high power impulse magnetron sputtering discharges

Jón Tómas Guðmundsson[1,2]

[1] Department of Space and Plasma Physics,
KTH Royal Institute of Technology, Stockholm, Sweden
[2] Science Institute, University of Iceland, Reykjavik, Iceland

Applied Materials
Sunnyvale, California
December 10, 2019

Introduction

- Magnetron sputtering has been a highly sucessfull technique that is essential in a number of industrial applications

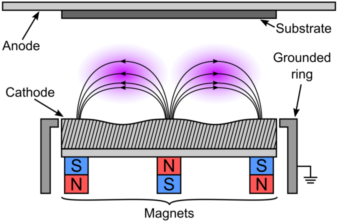

- A magnet is placed at the back of the cathode target with the pole pieces at the center and perimeter
- The magnetic field confines the energetic electrons near the cathode
- The electrons undergo numerous ionizing collisions before being lost to a grounded surface

The dc magnetron sputtering discharge

The dc magnetron sputtering discharge

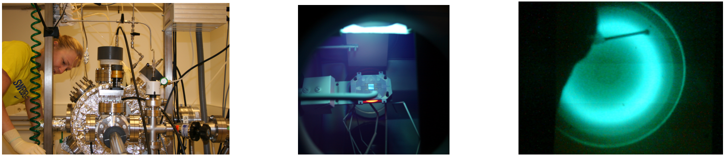

- Magnetron sputtering has been the workhorse of plasma based sputtering methods for over four decades
- Through the years there has been a continuous development of the magnetron sputtering processes to
  - increase the ionization of the sputtered vapor
  - improve target utilization
  - avoid target poisoning in reactive sputtering
  - increase deposition rates

The dc magnetron sputtering discharge

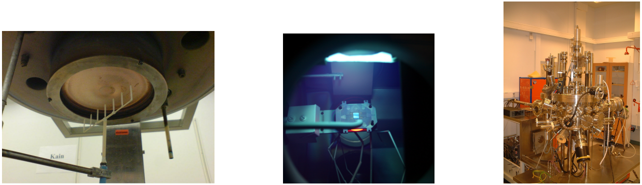

- For many applications a high degree of ionization of the sputtered vapor is desired
  - controlled ion bombardment of the growing film
  - ion energy can be – controlled by a negative bias applied to the substrate
  - collimation – enhanced step coverage

- Ionized flux of the sputtered material introduces an additional control parameter into the deposition process

The dc magnetron sputtering discharge

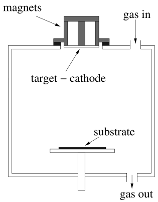

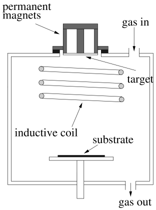

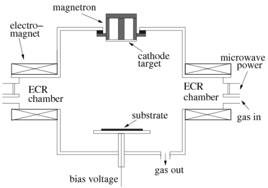

From Gudmundsson (2008), J. Phys.: Conf. Ser. **100** 082002

- In magnetron sputtering discharges increased ionized flux fraction is achieved by
  - a secondary discharge between the target and the substrate (rf coil or microwaves)
  - reshaping the geometry of the cathode to get more focused plasma (hollow cathode)
  - increasing the power to the cathode (high power pulse)
- Common to all highly ionized magnetron sputtering techniques is a very high density plasma

The high power impulse magnetron sputtering discharge

High power impulse magnetron sputtering discharge

- In a conventional dc magnetron discharge the power density is limited by the thermal load on the target
- Most of the ion bombarding energy is transformed into heat at the target
- In a HiPIMS discharge a high power pulse is supplied for a short period
  - low frequency
  - low duty cycle
  - low average power
- The high power pulsed magnetron sputtering discharge uses the same sputtering apparatus except the power supply

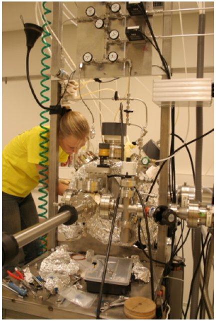

High power impulse magnetron sputtering discharge

- In dc magnetron sputtering the power density (plasma density) is limited by the thermal load on the target
- High power pulsed magnetron sputtering (HPPMS)
- High power impulse magnetron sputtering (HiPIMS)
  - a pulse of very high amplitude, an impulse, is applied to the cathode and a long pause exists between the pulses
- Modulated pulse power (MPP)
  - the initial stages of the pulse (few hundred μs) the power level is moderate (typical for a dcMS) followed by a high power pulse (few hundred μs up to a ms)

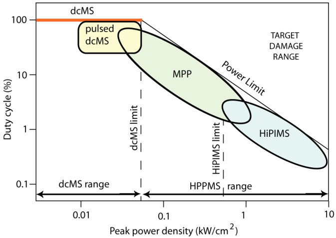

Gudmundsson et al. (2012) JVSTA **30** 030801

- Power density limits
  $p_t = 0.05$ kW/cm^2 dcMS limit
  $p_t = 0.5$ kW/cm^2 HiPIMS limit

High power impulse magnetron sputtering discharge

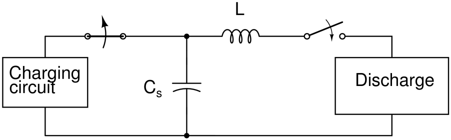

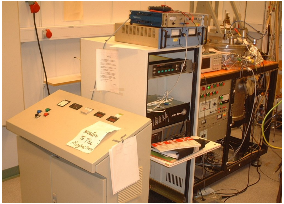

- The high power impulse magnetron sputtering (HiPIMS) discharge operates with a
  - Cathode voltage in the range of 500 – 2000 V
  - Current densities of 0.5 – 4 A/cm^2
  - Power densities in the range of 0.5 – 3 kW/cm^2
  - Average power 200 – 600 W
  - Frequency in the range of 50 – 5000 Hz
  - Duty cycle in the range of 0.5 – 5 %

High power impulse magnetron sputtering discharge

- The development of high power pulsed magnetron sputtering is traced to the Moscow Engineering and Physics Institute (MEPhI)
- The PhD thesis of Dimitry Mozgrin describes a high-current low-pressure quasistationary discharge in a magnetic field demonstrated for two configurations
  - a planar magnetron device
  - two hollow axisymmetric electrodes immersed in a cusp-shaped magnetic field
- The planar magnetron is operated at peak power of 200 kW (200 A) onto a 120 mm diameter target – peak power density of 1.8 kW/cm^2 and discharge current densities up to 25 A/cm^2 at a 10 Hz in a pre-ionized

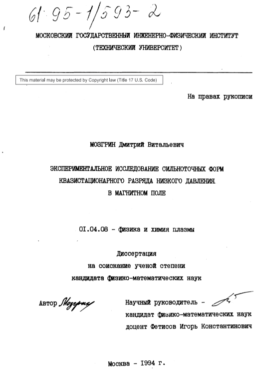

61·95-1/593-2

МОСКОВСКИЙ ГОСУДАРСТВЕННЫЙ ИНЖЕНЕРНО-ФИЗИЧЕСКИЙ ИНСТИТУТ
(ТЕХНИЧЕСКИЙ УНИВЕРСИТЕТ)

На правах рукописи

МОЗГРИН Дмитрий Витальевич

ЭКСПЕРИМЕНТАЛЬНОЕ ИССЛЕДОВАНИЕ СИЛЬНОТОЧНЫХ ФОРМ
КВАЗИСТАЦИОНАРНОГО РАЗРЯДА НИЗКОГО ДАВЛЕНИЯ
В МАГНИТНОМ ПОЛЕ

01.04.08 - физика и химия плазмы

Диссертация
на соискание ученой степени
кандидата физико-математических наук

Автор

Научный руководитель -
кандидат физико-математических наук
доцент Фетисов Игорь Константинович

Москва - 1994 г.

Mozgrin (1994) Ph.D. thesis, MEPhi

High power impulse magnetron sputtering discharge

- The original concept of a HiPIMS power supply, which was based on thyristor switches
- The length of the active pulse cannot be controlled, it is given by the time constant of the plasma impedance and the values of *C* and *L*
- The pulse repetition frequency is fixed by the ac line supply
- This type of power supply was used in the early demonstration of the HiPIMS technique performed at Linköping University

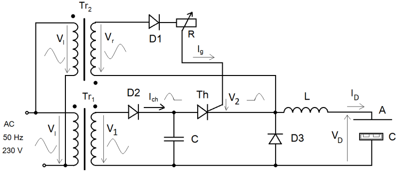

Based on Kouznetsov (2001) U.S. Patent no. 6,296,742

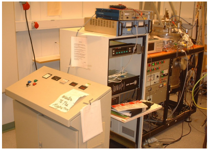

High power impulse magnetron sputtering discharge

- The discharge voltage V_D and current I_D for an argon discharge at 0.27 and 2.67 Pa with 150 mm diameter tantalum target driven by an early thyristor-based power supply
- We see an initial voltage peak in the kilovolt range which is followed by a drop in the voltage to several hundred volts
- The voltage then drops even further to values that are typical operating voltages for a dcMS discharge
- As the voltage drops, the discharge current increases up to a peak value followed by a gradual decay of the current

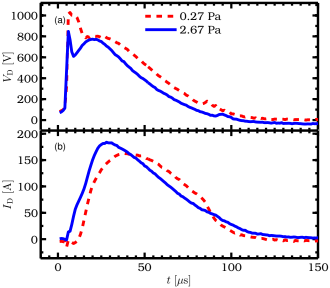

From Gudmundsson et al. (2002) SCT **161** 249

High power impulse magnetron sputtering discharge

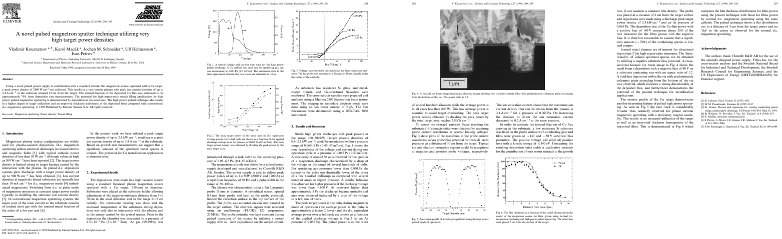

ELSEVIER
Surface and Coatings Technology 122 (1999) 290–293
SURFACE & COATINGS TECHNOLOGY
www.elsevier.nl/locate/surfcoat

A novel pulsed magnetron sputter technique utilizing very high target power densities

Vladimir Kouznetsov [a,*], Karol Macák [a], Jochen M. Schneider [a], Ulf Helmersson [a], Ivan Petrov [b]

[a] Department of Physics, Linköping University, SE-581 83 Linköping, Sweden
[b] Materials Science Department and Materials Research Laboratory, University of Illinois, Urbana, IL 61801, USA

Received 5 May 1999; accepted in revised form 28 May 1999

Abstract

Using a novel pulsed power supply in combination with a standard circular flat magnetron source, operated with a Cu target, a peak power density of 2800 W cm^{-2} was achieved. This results in a very intense plasma with peak ion current densities of up to 3.4 A cm^{-2} at the substrate situated 10 cm from the target. The ionized fraction of the deposited Cu flux was estimated to be approximately 70% from deposition rate measurements. The potential for high-aspect-ratio trench filling applications by high power pulsed magnetron sputtering is demonstrated by deposition in via-structures. The high power pulsed technique also results in a higher degree of target utilization and an improved thickness uniformity of the deposited films compared with conventional d.c. magnetron sputtering. © 1999 Published by Elsevier Science S.A. All rights reserved.

Keywords: Magnetron sputtering; Power density; Trench filling

1. Introduction

Magnetron plasma source configurations are widely used for plasma-assisted deposition. D.c. magnetron sputtering utilizes electrical discharges in crossed electric and magnetic fields [1] with typical cathode power densities of less than 50 W cm^{-2} although values as high as 300 W cm^{-2} have been reported [2]. The target power density is limited owing to target heating caused by the interaction with the plasma. In pulsed d.c. deposition systems glow discharge with a target power density of up to 900 W cm^{-2} has been obtained [3]. Ion current densities at negatively biased substrates are typically less than 10 mA cm^{-2} for d.c. magnetron mode [4] (unbalanced magnetron). Switching from d.c. to pulse mode of magnetron operation at constant target power results typically in doubling the substrate ion current density [5]. In conventional magnetron sputtering systems the major part of the ionic current at the substrate consists of ionized inert gas with the ionized metal fraction of the order of a few per cent [6].

In the present work we have utilized a peak target power density of up to 2.8 kW cm^{-2}, resulting in a peak ion current density of up to 3.4 A cm^{-2} at the substrate. Based on growth rate measurements we suggest that a significant amount of the sputtered metal species is ionized. The potential for Cu metallization applications is demonstrated.

2. Experimental details

The depositions were made in a high vacuum system using a standard balanced planar magnetron source operated with a Cu target, 150 mm in diameter. Substrates were placed at the substrate holder allowing adjustment of the target-to-substrate distance from 5 to 70 cm in the axial direction and in the range 0–15 cm radially. No intentional heating was done and the increased temperature of the substrates during deposition was only due to interaction with the plasma and to the energy carried by the arrival species. Prior to the deposition the chamber was evacuated to a pressure of 6.5×10^{-5} Pa (5×10^{-7} Torr). Ar gas (99.998%) was introduced through a leak valve to the operating pressure of 0.05–6.5 Pa (0.4–50 mTorr).

The magnetron cathode was driven by a pulsed power supply developed and manufactured by Chemfilt R&D AB, Sweden. The power supply is able to deliver peak power pulses of up to 2.4 MW (2000 V and 1200 A) at a repetition frequency of 50 Hz and a pulse width in the range of 50–100 μs.

The plasma was characterized using a flat Langmuir probe 15 mm in diameter. A cylindrical screen, spaced 0.5 mm from probe and kept at the probe potential, limited the collection surface to the top surface of the probe. The probe was mounted on-axis and parallel to the target surface. The electrical signals were recorded using an oscilloscope (FLUKE 123 scopemeter, 20 MHz). The probe potential was kept constant during pulsed operation of the source by utilizing a power supply with sufficient capacitance on the output circuit.

As substrates low resistance Si, glass, and metal-coated trench- and via-structured Si-wafers were employed. The cross-section samples were prepared and analyzed using a Micrion 2500 focused ion beam instrument. The imaging in secondary electron mode were done using an ion beam current of 5 pA. The film thicknesses were determined using a DEKTAK 3030 instrument.

3. Results and discussion

Stable high power discharges with peak powers in the range 100–500 kW (target powers densities of 0.6–2.8 kW cm^{-2}) could be maintained within a pressure range of 0.060–5 Pa (0.45–37 mTorr). Fig. 1 shows the time dependence of the voltage and current during one operation cycle at a pressure of 0.065 Pa (0.50 mTorr). A time delay of around 50 μs is observed for the ignition of a magnetron discharge characterized by a drop of the voltage in the range of several hundreds of volts. For sputtering gas pressures lower than 0.060 Pa the current in the pulse was drastically lower, of the order of a few hundred milliamps as compared with several hundred amps at higher pressure. A similar behavior was observed for higher pressures if the discharge voltage was lower than ∼800 V. At pressures higher than approximately 5 Pa the discharge became unstable and arcs were observed indicated by a drop of the voltage to a few tens of volts.

The peak target power in the pulse during magnetron mode of operation (the average power in the pulse is approximately a factor 2 lower) and the d.c. equivalent average power over a full cycle are shown as a function of the applied discharge voltage in Fig. 2 (at an Ar pressure of 0.065 Pa). The pulsed power is on the order of several hundred kilowatts while the average power is in all cases less than 800 W. This low average power is essential to avoid target overheating. The peak target power density obtained by dividing the peak power by the total target area reaches 2.8 kW cm^{-2}.

To assess the charged particles fluxes reaching the substrate *I–V* characteristics were obtained by acquiring probe current waveforms at several biasing voltages. Fig. 3 show plots of the maximum in the probe current waveforms versus probe bias potential for three different pressures at a distance of 10 cm from the target. Typical ion and electron saturation regions could be recognized at negative and positive probe voltages, respectively. The ion saturation current shows that the maximum ion current density that can be drawn from the plasma is 3.4 A cm^{-2} for a pressure of 0.065 Pa. On increasing the distance to 40 cm the ion saturation current decreased to 0.2 A cm^{-2} at the same pressure.

In order to estimate the ionized fraction of Cu flux arriving at the substrate, a low resistance Si substrate was fixed on the probe surface with conducting glue and films were grown at +140 and −50 V substrate bias potentials. The positive voltage will repel all positive ions with a kinetic energy of ≲140 eV. Comparing the resulting deposition rates yields a qualitative measure for the contribution of ions versus neutrals to the growth rate, if one assumes a constant film density. The probe was placed at a distance of 6 cm from the target surface and depositions were made using a discharge peak target power density of 2.8 kW cm^{-2} and an Ar pressure of 0.065 Pa. The deposition rate of the Cu film grown with a positive bias of 140 V comprises about 30% of the rate measured for the films grown with the negative bias. It is therefore reasonable to assume that a significant amount (∼70%) of the condensing species is ionized copper.

Ionized metal plasmas are of interest for directional deposition [7] in high-aspect-ratio structures. The 'directionality' of ionized sputtered species can be obtained by utilizing a negative substrate bias potential. A cross-sectional focused ion beam image in Fig. 4 shows the result from a deposition with a negative bias of 80 V on a substrate containing vias with an aspect ratio of 1.2. A void-free deposition within the via with predominately columnar grain extending from the bottom of the via was observed, which indicates a strong directionality of the deposited flux, and furthermore demonstrates the potential of the present technique for metallization applications.

The erosion profile of the Cu target demonstrates another interesting feature of pulsed high power sputtering. As seen in Fig. 5 the race track is considerably broader than normally observed for planar circular magnetron sputtering with a stationary magnet assembly. This results in an increased utilization of the target as well as an improved thickness homogeneity of the deposited films. This is demonstrated in Fig. 6 which compares the film thickness distributions for films grown using the present technique with those for films grown by normal d.c. magnetron sputtering using the same cathode. The pulsed technique shows a flat distribution out to a distance of 5 cm from the target center and no 'dip' in the center as observed for the normal d.c. magnetron sputtering.

Fig. 1. A typical voltage and current time trace for the high power pulsed discharge. A Cu cathode was used and the sputtering gas, Ar, was maintained at 0.065 Pa (0.5 mTorr). The maximum error in the time adjustment between the two traces are estimated to 10 μs.

Fig. 2. The peak target power in the pulse and the d.c. equivalent average power over a full cycle are shown as a function of the applied discharge voltage at an Ar pressure of 0.065 Pa (0.5 mTorr). The peak target power density was obtained by dividing the peak power by the total target area.

Fig. 3. Voltage–current probe characteristics for three operation pressures. The flat probe was mounted at a distance of 10 cm directly under the center of the cathode.

Fig. 4. A focused ion beam image (secondary electron image) showing two via-holes densely filled with predominately columnar grains extending from the bottom of the via. The aspect ratio is 1.2.

Fig. 5. An erosion profile of a Cu target sputtered using the high power pulsed mode of operation.

Fig. 6. The film thickness as a function of the radial distance from the center of the magnetron source for films grown using normal d.c. magnetron sputtering and high power pulsed sputtering. The substrates were placed 5 cm from the surface of the target.

Acknowledgements

The authors thank Chemfilt R&D AB for the use of the specially designed power supply, Fibics Inc. for the cross-section analysis and the Swedish National Board for Industrial and Technical Development, the Swedish Research Council for Engineering Sciences, and the US Department of Energy (DEFG0296ER45439) for financial support.

References

[1] R. Lehnert, Nucl. Fusion 11 (1971) 485.
[2] W.M. Posadowski, Vacuum 46 (1995) 1017.
[3] R. Gruen, Process and apparatus for coating conducting pieces using a pulsed glow discharge, US Patent 5015493, May 14, 1991.
[4] B. Window, N. Savvides, J. Vac. Sci. Technol. A 4 (1986) 453.
[5] S. Schiller, personal communication.
[6] I. Petrov, A. Myers, J.E. Greene, J.R. Abelson, J. Vac. Sci. Technol. A 12 (1994) 2846.
[7] S.M. Rossnagel, J. Hopwood, J. Vac. Sci. Technol. B 12 (1994) 449.

* Corresponding author. Tel.: +46-13-285-779; +46-8-531-84-000.
E-mail address: vlaku@yahoo.com (V. Kouznetsov)

0257-8972/99/$ – see front matter © 1999 Published by Elsevier Science S.A. All rights reserved.
PII: S0257-8972(99)00292-3

From Kouznetsov et al. (1999) SCT **122** 290

- This is the pulser unit used in the pionering work of Kouznetsov et al. (1999)

High power impulse magnetron sputtering discharge

- Modern concepts of pulsed power supplies utilize insulated-gate bipolar transistors (IGBTs) as high power switches
- Also, the previously used small capacitor *C* is substituted by a large capacitor bank composed of low-impedance electrolytic capacitors
- A typical circuit diagram of a HiPIMS power supply based on IGBT switches

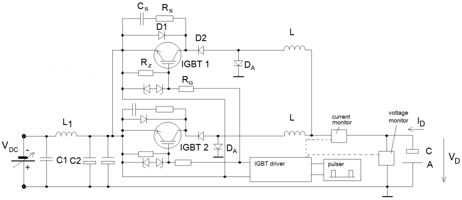

Hubička et al. (2020) in High Power Impulse Magnetron Sputtering Discharge, Elsevier, 2020

High power impulse magnetron sputtering discharge

- The discharge voltage V_D and current I_D for an argon discharge mixed with nitrogen at different flow rates and vanadium target
- The discharge is driven by an IGBT based power supply with a large capacitor bank
- The total gas pressure is 0.9 Pa, the argon flow rate is 40 sccm, the voltage pulse is 200 μs long and the pulse frequency is 100 Hz.

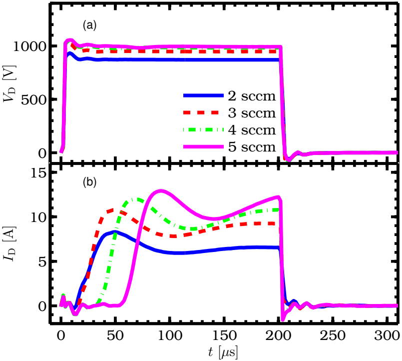

Hajihoseini and Gudmundsson (2017) JPD **50** 505302

High power impulse magnetron sputtering discharge

- Ar discharge with Ti target
- The initial peak in current results large flux of atoms from the target
- Collisions of the sputtered atoms with the working gas result in heating and expansion of the working gas – **rarefaction**
- A significant fraction of the sputtered atoms experience electron impact ionization (the ionization mean free path $\sim$ 1 cm) and are attracted back to the target to participate in the sputtering process – **self-sputtering**

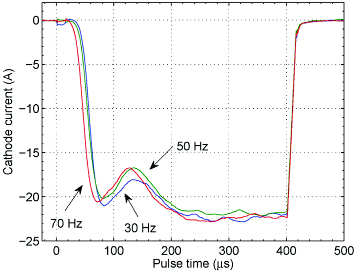

From Magnus et al. (2011) JAP **110** 083306

High power impulse magnetron sputtering discharge

- The initial phase has a contribution from the working gas ions, whereas the later phase has a strong contribution from self-sputtering at high voltage
- The current is generally characterized by an initial peak followed by a more or less stable current plateau (bottom current curves)
- In other cases it shows an initial peak followed by a second increase of the discharge current

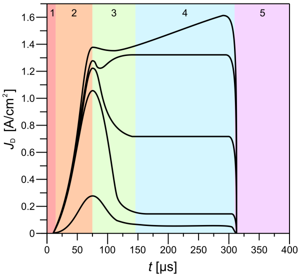

From Lundin et al. (2020), in High Power Impulse Magnetron Sputtering Discharge, Elsevier, 2020

High power impulse magnetron sputtering discharge

- We define

$$\Pi_{\rm ss} = \alpha_{\rm t}\beta_{\rm t} Y_{\rm ss}$$

where for the target material

  - $\alpha_{\rm t}$ the ionization probability
  - $\beta_{\rm t}$ the back-attraction probability
  - $Y_{\rm ss}$ the self-sputter yield
- $\Pi_{\rm ss} < 0.1$ – low self-sputtering and dcMS-like discharge
- $0.1 < \Pi_{\rm ss} < 1$ – partially self-sputtering discharge
- $\Pi_{\rm ss} > 1$ – self-sputtering runaway and $Y_{\rm ss} > 1/(\alpha\beta_{\rm t}) > 1$

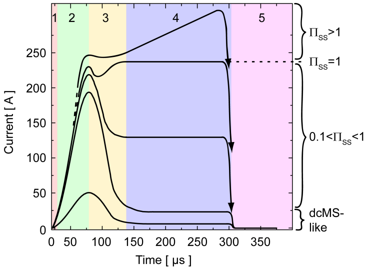

From Gudmundsson et al. (2012), JVSTA **30** 030801

High power impulse magnetron sputtering discharge

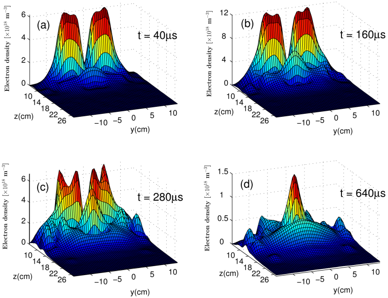

(After Bohlmark et al. (2005), IEEE Trans. Plasma Sci. **33** 346)

- Temporal and spatial variation of the electron density
- Ar discharge at 20 mTorr, Ti target, pulse length 100 μs
- The electron density in the substrate vicinity is of the order of $10^{18} - 10^{19}$ m^{-3} – ionization mean free path $\lambda_{\rm iz} \sim 1$ cm

High power impulse magnetron sputtering discharge

- The time averaged ion energy distribution for Ar^+ and Ti^+ ions
- The working gas pressure was 3 mTorr, pulse energy 3 J and 10 J and the target made of Ti
- The ion energy distribution is broad to over 100 eV
- About 50 % of the Ti^+ ions have energy > 20 eV

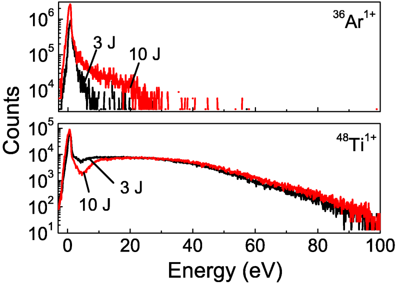

From Bohlmark et al. (2006) TSF **515** 1522

Thin film deposition

Thin film deposition

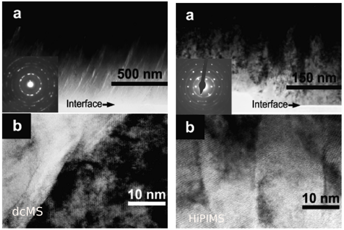

dc magnetron HiPIMS

After Alami et al. (2005) JVSTA, **23** 278

- In HiPIMS deposition, the high fraction of ionization of the sputtered species has been shown to lead to
  - the growth of smooth and dense films
  - enable control over their phase composition and microstructure
  - enhance mechanical and optical properties
  - improving film adhesion
  - enabling deposition of uniform films on complex-shaped substrates
- For optimization of HiPIMS thin film deposition processes, quantification and control of the fraction of ionization of the sputtered species are for obvious reasons key requirements

Thin film deposition

- The mass density is always higher when depositing with HiPIMS compared to dcMS at the same average power
- The surfaces are significantly smoother when depositing with HiPIMS compared to dcMS

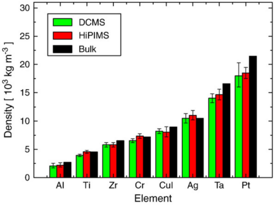

From Samuelsson et al. (2010) SCT **202** 591

Thin film deposition

- TiN as diffusion barriers for interconnects
- HiPIMS deposited films have significantly lower resistivity than dcMS deposited films on SiO_2 at all growth temperatures due to reduced grain boundary scattering
- Thus, ultrathin continuous TiN films with superior electrical characteristics and high resistance towards oxidation can be obtained with HiPIMS at reduced temperatures

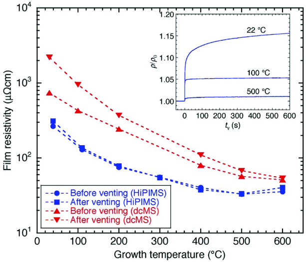

From Magnus et al. (2012) IEEE EDL **33** 1045

Thin film deposition

- The effect of ionization fraction on the epitaxial growth of Cu film on Cu(111) substrate explored using Molecular Dynamics simulation
- Three deposition methods
    - thermal evaporation, fully neutral
    - dcMS, 50 % ionized
    - HiPIMS, 100 % ionized
- Higher ionization fraction of the deposition flux leads to smoother surfaces by two major mechanisms
    - decreasing clustering in the vapor phase
    - bicollision of high energy ions at the film surface that prevents island growth to become dominant

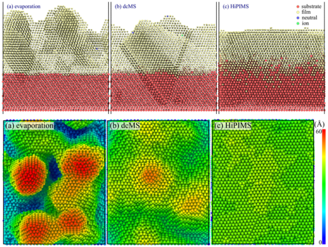

After Kateb et al. (2019) JVSTA, **37** 031306

Thin film deposition

- There have been a number of reports demonstrating the lower deposition rate in HiPIMS when compared to dcMS operated at the same average power
- Samuelsson et al. (2010) compared the deposition rates from eight metal targets (Ti, Cr, Zr, Al, Cu, Ta, Pt, Ag) in pure Ar for both dcMS and HiPIMS discharges applying the same average power
- They observed that the HiPIMS deposition rates were in the range of 30 – 85% of the dcMS rates depending on target material.

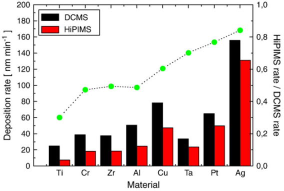

From Samuelsson et al. (2010) SCT **202** 591

Electron power absorption in magnetron sputtering discharges

Introduction

- The conventional wisdom is that plasma generation in magnetron sputtering discharges is based on the supply of energy via secondary electrons (SEs) accelerated from the target
- However, one of the remaining fundamental questions is **how power is absorbed by the electrons in the magnetron sputtering discharge**

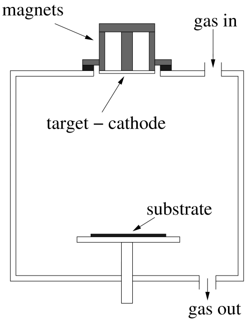

dc magnetron sputtering discharge

dc magnetron sputtering discharge

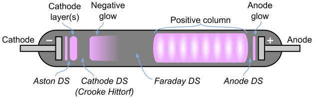

T. J. Petty, LPGP, Université Paris Sud

- A dc discharge with a cold cathode is sustained by secondary electron emission from the cathode by ion bombardment
- The discharge current at the target consists of electron current I_e and ion current I_i or

  $$I_\mathrm{D} = I_\mathrm{e} + I_\mathrm{i} = I_\mathrm{i}(1 + \gamma_\mathrm{SE})$$

  where γ_SE is the secondary electron emission coefficient
- Note that $\gamma_\mathrm{SE} \sim 0.05 - 0.2$ for most metals, so at the target, the dominating fraction of the discharge current is ion current

dc magnetron sputtering discharge

- These secondary electrons are accelerated in the cathode dark space – referred to as primary electrons
- They must produce sufficient number of ions to release more electrons from the cathode
- The number of electron-ion pairs created by each secondary electron is then

$$\mathcal{N} \approx \frac{V_\mathrm{D}}{\mathcal{E}_\mathrm{c}}$$

where $\mathcal{E}_\mathrm{c}$ is the energy loss per electron-ion pair created

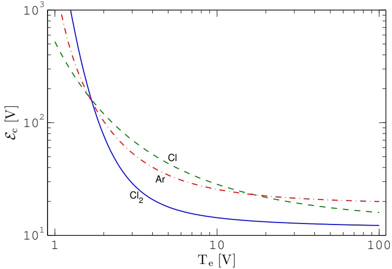

dc magnetron sputtering discharge

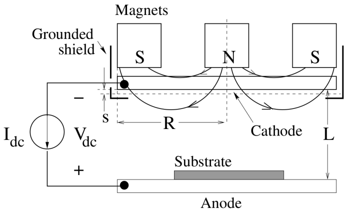

- To account for the electrons that are not trapped we define an effective secondary electron emission coefficient

$$\gamma_{\mathrm{SE,eff}} = m\epsilon_{\mathrm{e}}(1-r)\gamma_{\mathrm{SE}}$$

- ϵ_{e} is the fraction of the electron energy that is used for ionization before being lost
- m is a factor that accounts for secondary electrons ionizing in the sheath
- r is the recapture probability of secondary electrons

dc magnetron sputtering discharge

- To sustain the discharge the condition

  $$\gamma_{\mathrm{SE,eff}}\mathcal{N} = 1$$

  has to be fulfilled
- This defines the minimum voltage to sustain the discharge as

  $$V_{\mathrm{D,min}} = \frac{\mathcal{E}_{\mathrm{c}}}{\beta\gamma_{\mathrm{SE,eff}}}$$

  referred to as Thornton equation
  - β is the fraction of ions that return to the cathode

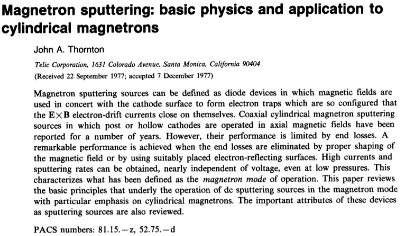

Magnetron sputtering: basic physics and application to cylindrical magnetrons

John A. Thornton

Telic Corporation, 1631 Colorado Avenue, Santa Monica, California 90404

(Received 22 September 1977; accepted 7 December 1977)

Magnetron sputtering sources can be defined as diode devices in which magnetic fields are used in concert with the cathode surface to form electron traps which are so configured that the $\mathbf{E}\times\mathbf{B}$ electron-drift currents close on themselves. Coaxial cylindrical magnetron sputtering sources in which post or hollow cathodes are operated in axial magnetic fields have been reported for a number of years. However, their performance is limited by end losses. A remarkable performance is achieved when the end losses are eliminated by proper shaping of the magnetic field or by using suitably placed electron-reflecting surfaces. High currents and sputtering rates can be obtained, nearly independent of voltage, even at low pressures. This characterizes what has been defined as the *magnetron mode* of operation. This paper reviews the basic principles that underly the operation of dc sputtering sources in the magnetron mode with particular emphasis on cylindrical magnetrons. The important attributes of these devices as sputtering sources are also reviewed.

PACS numbers: 81.15.−z, 52.75.−d

Thornton (1978) JVST **15**(2) 171

dc magnetron sputtering discharge

- The basic assumption is that acceleration across the sheath is the main source of energy for the electrons
- Above breakdown the parmeters m, β, $\epsilon_{\rm e}$ and r can vary with the applied voltage
- We can rewrite the Thornton equation for any voltage

$$\frac{1}{V_{\rm D}} = \frac{\beta m \epsilon_{\rm e}(1-r)}{\mathcal{E}_{\rm c}}\gamma_{\rm SE}$$

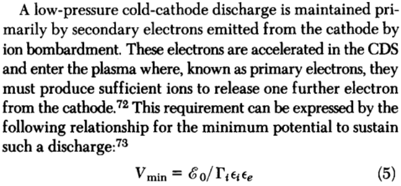

A low-pressure cold-cathode discharge is maintained primarily by secondary electrons emitted from the cathode by ion bombardment. These electrons are accelerated in the CDS and enter the plasma where, known as primary electrons, they must produce sufficient ions to release one further electron from the cathode.[72] This requirement can be expressed by the following relationship for the minimum potential to sustain such a discharge:[73]

$$V_{\rm min} = \mathscr{E}_0/\Gamma_i\epsilon_i\epsilon_e \qquad (5)$$

Thornton (1978) JVST **15**(2) 171

dc magnetron sputtering discharge

- A plot of the inverse discharge voltage $1/V_\mathrm{D}$ against γ_SE should then give a straight line through the origin
- Depla et al. measured the discharge voltage for a 5 cm diameter target for Ar working gas for 18 different target materials
- Since all the data is taken in the same magnetron, at same current and pressure, the discharge parameters parmeters m, β, ϵ_e and $\mathcal{E}_\mathrm{c}$ are independent of γ_SE

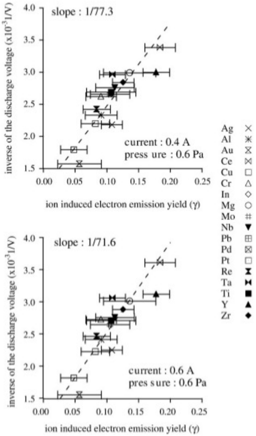

From Depla et al. (2009) TSF **517** 2825

dc magnetron sputtering discharge

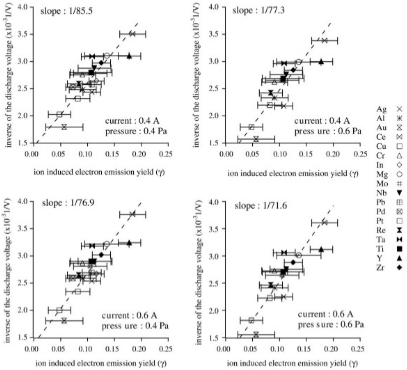

From Depla et al. (2009) TSF **517** 2825

- $1/V_\mathrm{D}$ against γ_SE for gas pressures of 0.4 and 0.6 Pa and discharge currents 0.4 A and 0.6 A
- It can be seen that a straight line indeed results, but that it does not pass through the origin

dc magnetron sputtering discharge

- We here propose that the intercept is due to Ohmic heating
- We can now write the inverse discharge voltage $1/V_{\mathrm{D}}$ in the form of a generalized Thornton equation

$$\frac{1}{V_{\mathrm{D}}} = \underbrace{\frac{\beta \epsilon_{\mathrm{e}}^{\mathrm{H}} m(1-r)(1-\delta_{\mathrm{IR}})}{\mathcal{E}_c^{\mathrm{H}}}}_{a} \gamma_{\mathrm{SE}} + \underbrace{\frac{\epsilon_{\mathrm{e}}^{\mathrm{C}} \langle I_{\mathrm{e}}/I_{\mathrm{D}}\rangle_{\mathrm{IR}} \delta_{\mathrm{IR}}}{\mathcal{E}_c^{\mathrm{C}}}}_{b}$$

or

$$\frac{1}{V_{\mathrm{D}}} = a\gamma_{\mathrm{SE}} + b$$

- We associate *a* with hot electrons e^{H}, sheath acceleration
- We associate *b* with the Ohmic heating process and cold electrons e^{C}

dc magnetron sputtering discharge

- The figure shows schematically the magnetic field lines and the electric equipotential surfaces above the racetrack
- A potential V_{SH} falls over the sheath, and the rest of the applied voltage, $V_{\mathrm{IR}} = V_{\mathrm{D}} - V_{\mathrm{SH}}$, falls across the extended pre-sheath, the ionization region (IR), $\delta_{\mathrm{IR}} = V_{\mathrm{IR}}/V_{\mathrm{D}}$
- Ohmic heating, the dissipation of locally deposited electric energy $\mathbf{J}_{\mathrm{e}} \cdot \mathbf{E}$ to the electrons in the plasma volume outside the sheath

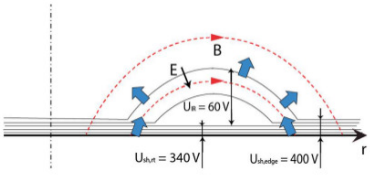

From Brenning et al. (2016) PSST **25** 065024

dc magnetron sputtering discharge

I_D (A)	p (Pa)	Slope k	Intercept I	$\delta_{IR} = U_{IR}/U_D$
0.4	0.4	0.0117	0.001 45	0.19
0.4	0.6	0.0129	0.001 20	0.16
0.6	0.4	0.0130	0.001 30	0.17
0.6	0.6	0.0140	0.001 10	0.15

- It follows that the fraction of the total ionization that is due to Ohmic heating can be obtained directly from the line fit parameters *a* and *b*
- This can be written as a function of only the secondary electron yield $\gamma_{\rm SE}$

$$\frac{\iota_{\rm Ohmic}}{\iota_{\rm total}} = \frac{b}{a\gamma_{\rm SE} + b}$$

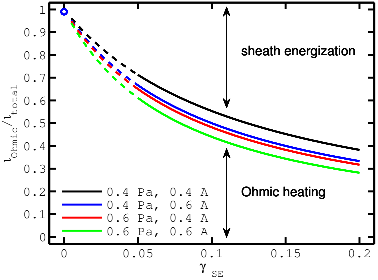

From Brenning et al. (2016) PSST **25** 065024

dc magnetron sputtering discharge

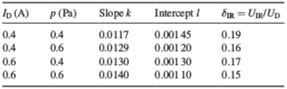

I_D (A)	p (Pa)	Slope k	Intercept l	$\delta_{IR} = U_{IR}/U_D$
0.4	0.4	0.0117	0.001 45	0.19
0.4	0.6	0.0129	0.001 20	0.16
0.6	0.4	0.0130	0.001 30	0.17
0.6	0.6	0.0140	0.001 10	0.15

- The fraction of the discharge voltage that falls over the ionization region

$$\delta_{\rm IR} = \frac{V_{\rm IR}}{V_{\rm D}}$$

can be estimated from

$$b = \frac{\epsilon_{\rm e}^{\rm C} \langle I_{\rm e}/I_{\rm D}\rangle_{\rm IR} \delta_{\rm IR}}{\mathcal{E}_c^{\rm C}}$$

- We assume

$$\epsilon_{\rm e}^{\rm C} = 0.8, \quad \langle I_{\rm e}/I_{\rm D}\rangle_{\rm IR} \approx 0.5,$$

and

$$\mathcal{E}_c^{\rm C} = 53.5~{\rm V} \;\; {\rm for} \;\; T_{\rm e} = 3~{\rm V}$$

which gives

$$\delta_{\rm IR} = 0.15 - 0.19$$

- 15 - 19 % of the applied discharge voltage fall over the ionization region

dc magnetron sputtering discharge

- Recent measurements have revealed strong electric fields parallel and perpendicular to the target of a dc magnetron sputtering discharge
- The largest **E**-fields result from a double layer structure at the leading edge of an ionization zone
- It is suggested that the double layer plays a crucial role in the energization of electrons since electrons can gain several tens of eV when crossing the double layer

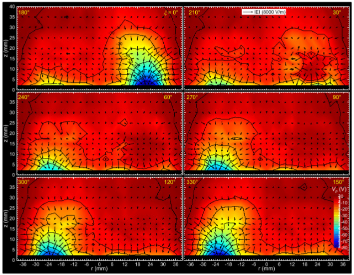

From Panjan and Anders (2017) JAP **121** 063302

dc magnetron sputtering discharge

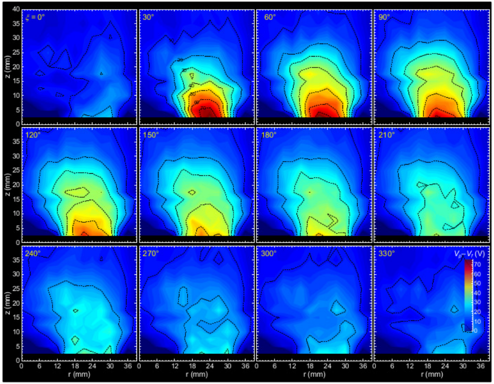

From Panjan and Anders (2017) JAP **121** 063302

- The distribution of $V_\mathrm{p} - V_\mathrm{f} \propto \langle E \rangle$ in the $r - z$ plane for a dc magnetron sputtering discharge operated at 270 V and 0.27 Pa

dc magnetron sputtering discharge

- Electrons gain energy when they encounter an electric field – a potential gradient, such as the field in the double layer
- The electron heating power $\mathbf{J}_\mathrm{e} \cdot \mathbf{E}$ is associated with an acceleration of electrons in the electric field – this electron energization in a double layer is Ohmic heating

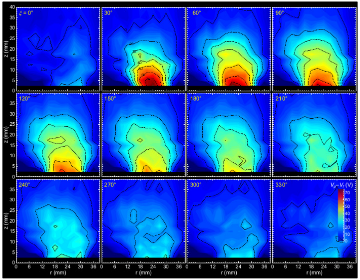

From Panjan and Anders (2017) JAP **121** 063302

Ionization region model studies of HiPIMS discharges

Ionization region model of HiPIMS

- The ionization region model (IRM) was developed to improve the understanding of the plasma behaviour during a HiPIMS pulse and the afterglow
- The main feature of the model is that an ionization region (IR) is defined next to the race track
- The IR is defined as an annular cylinder with outer radii $r_{\rm c2}$, inner radii $r_{\rm c1}$ and length $L = z_2 - z_1$, extends from z_1 to z_2 axially away from the target

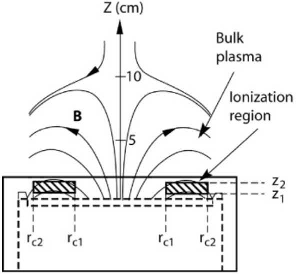

The definition of the volume covered by the IRM

From Raadu et al. (2011) PSST **20** 065007

Ionization region model of HiPIMS

- The temporal development is defined by a set of ordinary differential equations giving the first time derivatives of
  - the electron energy
  - the particle densities for all the particles
- The species assumed in the of-IRM are
  - cold electrons e^{C} (Maxwellian), hot electrons e^{H} (sheath acceleration)
  - argon atoms $\mathrm{Ar}(3s^2 3p^6)$, warm argon atoms in the ground state Ar^{W}, hot argon atoms in the ground state Ar^{H}, Ar^{m} ($1s_5$ and $1s_3$) (11.6 eV), argon ions Ar^{+} (15.76 eV)
  - titanium atoms $\mathrm{Ti}(\mathrm{a}\,{}^3\mathrm{F})$, titanium ions Ti^{+} (6.83 eV), doubly ionized titanium ions Ti^{2+} (13.58 eV)
  - aluminium atoms $\mathrm{Al}({}^2\mathrm{P}_{1/2})$, aluminium ions Al^{+} (5.99 eV), doubly ionized aluminium ions Al^{2+} (18.8 eV)

Detailed model description is given in Huo et al. (2017) JPD **50** 354003

Ionization region model of HiPIMS

- The model is constrained by experimental data input and fitted to reproduce the measured discharge current and voltage curves, $I_{\mathrm{D}}(t)$ and $V_{\mathrm{D}}(t)$, respectively
- Two model fitting parameters were found to be sufficient for a discharge with Al target
    - V_{IR} accounts for the power transfer to the electrons
    - β is the probability of back-attraction of ions to the target

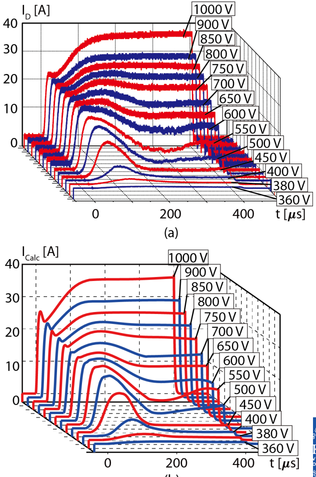

(a)

(b)

From Huo et al. (2017) JPD **50** 354003

Experimental data from Anders et al. (2007) JAP **102** 113303

Ionization region model of HiPIMS

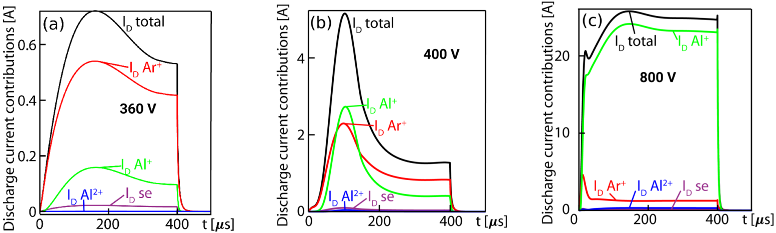

- A **non-reactive** discharge with 50 mm diameter Al target
- Current composition at the target surface

From Huo et al. (2017) JPD **50** 354003

Experimental data from Anders et al. (2007) JAP **102** 113303

Ionization region model of HiPIMS

- When the discharge is operated at 400 V the contributions of Al^+ and Ar^+-ions to the discharge current are very similar
- At 800 V Al^+-ions dominate the discharge current (**self-sputtering**) while the contribution of Ar^+ is below 10 % except at the initiation of the pulse

From Huo et al. (2017) JPD **50** 354003

Experimental data from Anders et al. (2007) JAP **102** 113303

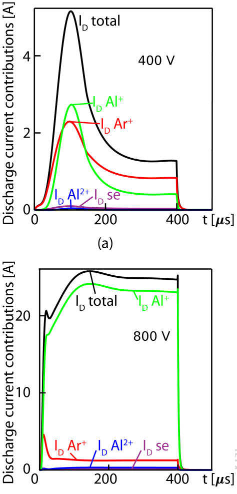

(a)

(b)

Ionization region model of HiPIMS

- A primary current $I_{\rm prim}$ is defined as ions of the working gas, here Ar^+, that are ionized for the first time and then drawn to the target
- This is the dominating current in dc magnetron sputtering discharges
- This current has a critical upper limit

$$I_{\rm crit} = S_{\rm RT} e p_{\rm g} \sqrt{\frac{1}{2\pi m_{\rm g} k_{\rm B} T_{\rm g}}} = S_{\rm RT} e n_{\rm g} \sqrt{\frac{k_{\rm B} T_{\rm g}}{2\pi m_{\rm g}}}$$

- Discharge currents $I_{\rm D}$ above $I_{\rm crit}$ are only possible if there is some kind of recycling of atoms that leave the target, become subsequently ionized and then are drawn back to the target

Anders et al. (2012) JPD **45** 012003

Huo et al. (2014) PSST **23** 025017

Ionization region model of HiPIMS

- For the 50 mm diameter Al target the critical current is $I_{\mathrm{crit}} \approx 7$ A
- The experiment is operated from far below I_{crit} to high above it, up to 36 A.
- With increasing current I_{prim} gradually becomes a very small fraction of the total discharge current I_{D}
- The current becomes mainly carried by singly charged Al^{+}-ions, meaning that **self-sputter recycling** or the current $I_{\mathrm{SS-recycle}}$ dominates

From Huo et al. (2017) JPD **50** 354003

Experimental data from Anders et al. (2007) JAP **102** 113303

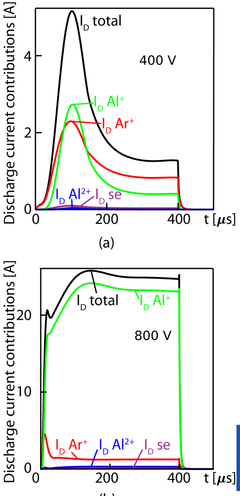

(a)

(b)

Ionization region model of HiPIMS

- For discharges with Ti target the peak current is far above the critical current (up to 650 A, while $I_{\mathrm{crit}} \approx 19$ A)
- However, this discharge shows close to a 50/50 combination of **self-sputter recycling** $I_{\mathrm{SS-recycle}}$ and **working gas-recycling** $I_{\mathrm{gas-recycle}}$
- Almost 2/3 of the current to the target is here carried by Ar$^+$ and Ti^{2+}-ions, which both can emit secondary electrons upon target bombardment, and this gives a significant sheath energization

From Huo et al. (2017) JPD **50** 354003

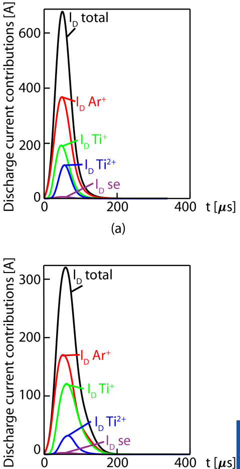

(a)

(b)

Ionization region model of HiPIMS

- Recall that singly charged metal ions cannot create the secondary electrons – for metal self-sputtering ($\gamma_{\rm SE}$ is practically zero)
- The first ionization energies of many metals are insufficient to overcome the workfunction of the target material
- For the discharge with Al target operated at high voltage, self-sputter dominated, the effective secondary electron emission is essentially zero

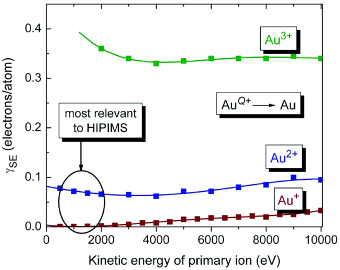

From Anders (2008) APL **92** 201501

Ionization region model of HiPIMS

- **Reactive** HiPIMS
- Ar/O_2 discharge with Ti target
- For this system $I_{\mathrm{crit}} \approx 5$ A
- In the metal mode Ar^+ and Ti^+-ions contribute roughly equally to the current – combined **self-sputter recycling** and **working gas recycling**
- In the poisoned mode the current increaes and Ar^+-ions dominate the current – **working gas recycling**

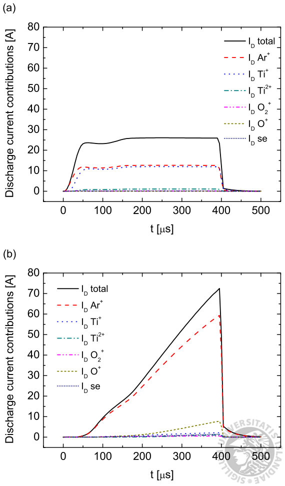

From Gudmundsson et al. (2016) PSST **25**(6) 065004

Ionization region model of HiPIMS

- For the Al target, Ohmic heating is in the range of 87 % (360 V) to 99 % (1000 V)
- The domination of Al^{+}-ions, which have zero secondary electron emission yield, has the consequence that there is negligible sheath energization
- The ionization threshold for twice ionized Al^{2+}, 18.8 eV, is so high that few such ions are produced

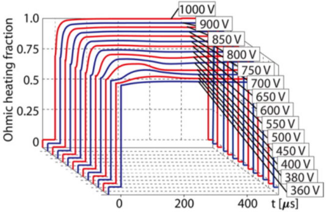

From Huo et al. (2017) JPD **50** 354003

Ionization region model of HiPIMS

- For a Ti target Ohmic heating is about 92 %
    - Both Ar^{+} and Ti^{2+}-ions contribute to creation of secondary electrons
- For Ti target in Ar/O_2 mixture
    - In the metal mode Ohmic heating is found to be 90 % during the plateau phase of the discharge pulse
    - For the poisoned mode Ohmic heating is 70 % with a decreasing trend, at the end of the pulse

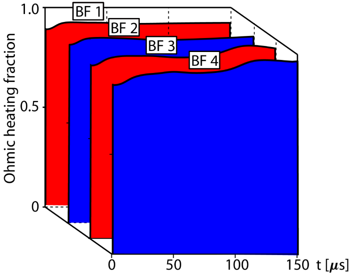

From Huo et al. (2017) JPD **50** 354003

Ionization region model of HiPIMS

- Ohmic heating is also very significant in dc magnetron sputtering discharges
- The relative contributions to the total ionization ι_{total} due to Ohmic heating, ι_{Ohmic}, and sheath energization, ι_{sheath}
- A blue circle marks the HiPIMS study modelled by Huo et al. (2013)
- Note that this HiPIMS case $\gamma_{\text{SE,eff}}$ is consistent with the dcMS cases

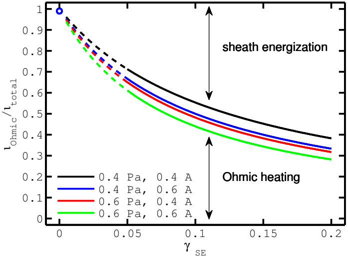

From Brenning et al. (2016) PSST **25** 065024

The generalized recycling model

Generalized recycling

- We have seen that the discharge current is composed of
  - working gas ions
  - ions of the sputtered material
- The total discharge current is

$$I_{\mathrm{D}} = I_{\mathrm{prim}} + I_{\mathrm{gas-recycle}} + I_{\mathrm{SS}}$$

- We have also seen that a large fraction of these ions have to be recycled

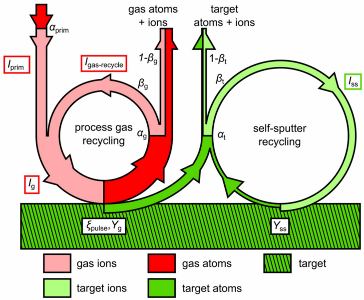

From Brenning et al. (2017) PSST **26** 125003

Generalized recycling

- A working gas-sputtering parameter

$$\pi_{\mathrm{g}} = \alpha_{\mathrm{g}}\beta_{\mathrm{g}}\xi_{\mathrm{pulse}}$$

where

  - α_{g} is ionization probability
  - β_{g} is back attraction probability
  - $\xi_{\mathrm{pulse}} = 1$ is return fraction in a pulse
- The total current carried by working gas ions

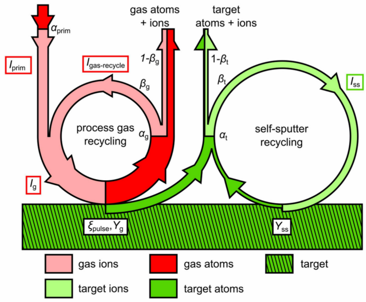

$$I_{\mathrm{g}} = I_{\mathrm{prim}} + I_{\mathrm{gas-recycle}} = I_{\mathrm{prim}}\left(1 + \frac{\pi_{\mathrm{g}}}{1 - \pi_{\mathrm{g}}}\right)$$

From Brenning et al. (2017) PSST **26** 125003

Generalized recycling

- The total self-sputter current is

$$I_{\mathrm{SS}} = I_{\mathrm{g}} \left(\frac{Y_{\mathrm{g}}}{Y_{\mathrm{SS}}} \frac{\pi_{\mathrm{SS}}}{1 - \pi_{\mathrm{SS}}} \right)$$

where the self-sputter parameter is

$$\pi_{\mathrm{SS}} = \alpha_{\mathrm{t}} \beta_{\mathrm{t}} Y_{\mathrm{SS}}$$

- The total discharge current is

$$I_{\mathrm{D}} = I_{\mathrm{prim}} + I_{\mathrm{gas-recycle}} + I_{\mathrm{SS}}$$

$$= I_{\mathrm{prim}} \left(1 + \frac{\pi_{\mathrm{g}}}{1 - \pi_{\mathrm{g}}} \right) \left(1 + \frac{Y_{\mathrm{g}}}{Y_{\mathrm{SS}}} \frac{\pi_{\mathrm{SS}}}{1 - \pi_{\mathrm{SS}}} \right)$$

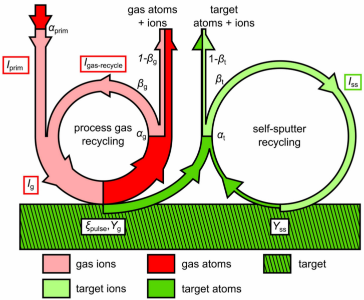

From Brenning et al. (2017) PSST **26** 125003.

Generalized recycling

- The discharge current

$$I_{\mathrm{D}} = I_{\mathrm{prim}} \Pi_{\mathrm{gas-recycle}} \Pi_{\mathrm{SS-recycle}}$$

- I_{prim} is the seed current that acts as a seed to the whole discharge current and has an upper limit I_{crit}
- $I_{\mathrm{prim}} \Pi_{\mathrm{gas-recycle}}$ is the seed current for the self-sputter process
- If $\pi_{\mathrm{SS}} > 1$ the discharge goes into SS-runaway

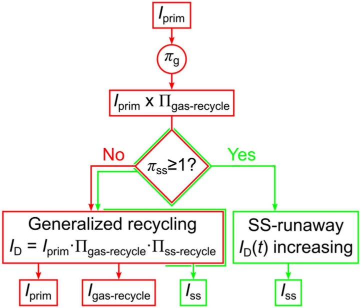

I_{prim}

π_{g}

I_{prim} x $\Pi_{\mathrm{gas\text{-}recycle}}$

$\pi_{\mathrm{ss}} \geq 1?$

No

Yes

Generalized recycling

$I_{\mathrm{D}} = I_{\mathrm{prim}} \cdot \Pi_{\mathrm{gas\text{-}recycle}} \cdot \Pi_{\mathrm{ss\text{-}recycle}}$

SS-runaway

$I_{\mathrm{D}}(t)$ increasing

I_{prim}

$I_{\mathrm{gas\text{-}recycle}}$

I_{ss}

I_{ss}

From Brenning et al. (2017) PSST **26** 125003

Generalized recycling

- Recycling map
- A graph in which the ion current mix of $I_{\rm prim}$, $I_{\rm gas-recycle}$, and $I_{\rm SS}$ to the target in a magnetron discharge is defined by a point
- The value of $I_{\rm prim}/I_{\rm D} = 39$ %, can be read on the diagonal lines ($Y_{\rm SS} = 0.5$)
- $I_{\rm prim}/I_{\rm D} \geq 0.85$ defines the dcMS regime
- For $I_{\rm SS}/I_{\rm D} > 0.5$ we have the SS-recycle dominated range A
- For $I_{\rm gas-recycle}/I_{\rm D} > 0.5$ we have the gas-recycle dominated range B

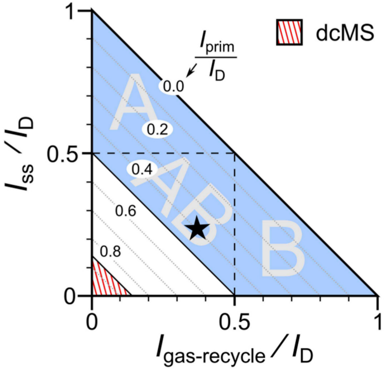

From Brenning et al. (2017) PSST **26** 125003

Generalized recycling

- The discharge with Al target moves from the dcMS regime to the HiPIMS discharge regime with increased discharge voltage – **type A**
- A discharge with carbon target jumps from the dcMS regime to the HiPIMS regime – both SS recycling and working gas recycling play a role – intermediate **type AB**

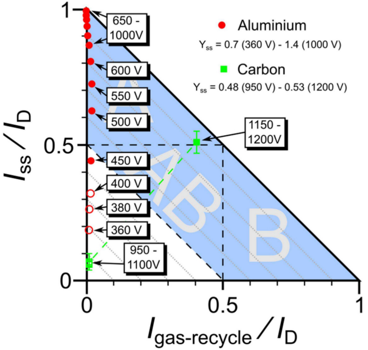

From Brenning et al. (2017) PSST **26** 125003

Generalized recycling

- Recycling map for five different targets with varying self-sputter yield
  - Cu – $Y_{\rm SS} = 2.6$
  - Al – $Y_{\rm SS} = 1.1$
  - Ti – $Y_{\rm SS} = 0.7$
  - C – $Y_{\rm SS} = 0.5$
  - TiO_2 – $Y_{\rm SS} = 0.04 - 0.25$
- For very high self-sputter yields $Y_{\rm SS} > 1$, the discharges above $I_{\rm crit}$ are of **type A** with dominating **SS-recycling**
- For very low self-sputter yields $Y_{\rm SS} < 0.2$, the discharges above $I_{\rm crit}$ are of **type B** with dominating **working gas recycling**

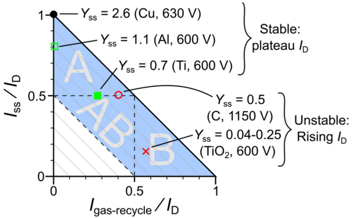

From Brenning et al. (2017), PSST **26** 125003

Generalized recycling

- Recycling loops
- Discharge with Al target – SS recycling dominates
  - high self sputter yield
- Reactive discharge with TiO_2 target – working gas recycling dominates
  - low self sputter yield

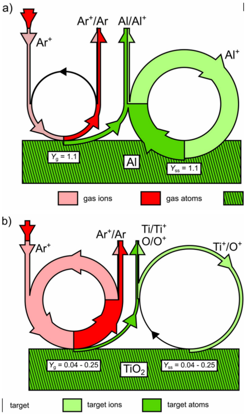

From Brenning et al. (2017) PSST **26** 125003

HiPIMS - Voltage - Current - time

- For Ar/O_2 discharge with Ti target
- At high frequencies, oxide is not able to form between pulses, and **self-sputtering recycling** by Ti^+-ions is the dominant process
- At low frequency, the long off-time results in an oxide layer being formed (TiO_2) on the target surface and **working gas recycling dominates** – triangular current waveform

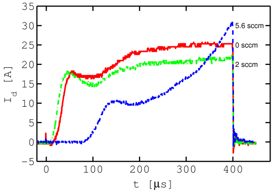

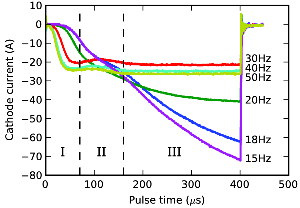

From Gudmundsson (2016), PPCF **58** 014002

Magnus et al. (2012), JVSTA **30** 050601

Summary

Summary

- It has been demonstrated that Ohmic heating of the electrons can play a significant role in conventional dc magnetron sputtering discharges
- We used a ionization region model to explore the plasma composition and the electron heating mechanism in a high power impulse magnetron sputtering (HiPIMS) discharge
    - For high currents the discharge with Al target develops almost pure **self-sputter recycling**, while the discharge with Ti target exhibits close to a 50/50 combination of **self-sputter recycling** and **working gas-recycling**
    - The fraction of the total electron heating that is attributable to Ohmic heating is over 90 % in the HiPIMS discharge

Summary

- For very high self-sputter yields, above approximately $Y_{\mathrm{SS}} \approx 1$, the discharges above I_{crit} are of type A with
  - dominating SS-recycling
  - very little secondary electron emission
  - little sheath energization of electrons
- For very low self-sputter yields, below approximately $Y_{\mathrm{SS}} \approx 0.2$, the discharges above I_{crit} are of type B with
  - dominating working gas recycling
  - significant secondary electron emission
  - significant sheath energization of electrons.

Thank you for your attention

The slides can be downloaded at

`http://langmuir.raunvis.hi.is/~tumi/ranns.html`

The work is in collaboration with

- Dr. Daniel Lundin, Université Paris-Sud, Orsay, France
- Prof. Nils Brenning, KTH Royal Institite of Technology, Stockholm, Sweden
- Dr. Michael A. Raadu, KTH Royal Institite of Technology, Stockholm, Sweden
- Prof. Tiberu Minea, Université Paris-Sud, Orsay, France

and the project has been funded by

- Icelandic Research Fund Grant Nos. 130029, 196141
- Swedish Government Agency for Innovation Systems (VINNOVA) contract no. 2014-04876

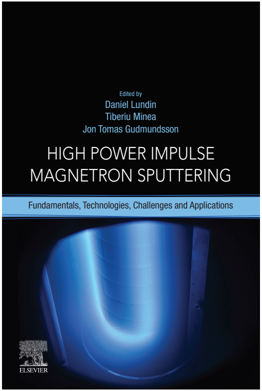

Edited by
Daniel Lundin
Tiberiu Minea
Jon Tomas Gudmundsson

HIGH POWER IMPULSE
MAGNETRON SPUTTERING

Fundamentals, Technologies, Challenges and Applications

ELSEVIER

- A comprehensive description of the HiPIMS process from the fundamental discharge physics to applications
- Shows how the HiPIMS process parameters can be adjusted to control film growth and thereby tune film properties, including hardness, refractive index, and residual stress

References

Alami, J., P. O. A. Petersson, D. Music, J. T. Gudmundsson, J. Bohlmark, and U. Helmersson (2005). Ion-assisted physical vapor deposition for enhanced film deposition on non-flat surfaces. *Journal of Vacuum Science and Technology A 23*(2), 278–280.

Anders, A. (2008). Self-sputtering runaway in high power impulse magnetron sputtering: The role of secondary electrons and multiply charged metal ions. *Applied Physics Letters 92*(20), 201501.

Anders, A. (2011). Discharge physics of high power impulse magnetron sputtering. *Surface and Coatings Technology 205*, S1–S9.

Anders, A., J. Andersson, and A. Ehiasarian (2007). High power impulse magnetron sputtering: Current-voltage-time characteristics indicate the onset of sustained self-sputtering. *Journal of Applied Physics 102*(11), 113303.

Anders, A., J. Čapek, M. Hála, and L. Martinu (2012). The 'recycling trap': a generalized explanation of discharge runaway in high-power impulse magnetron sputtering. *Journal of Physics D: Applied Physics 45*(1), 012003.

Bohlmark, J., J. T. Gudmundsson, J. Alami, M. Lattemann, and U. Helmersson (2005). Spatial electron density distribution in a high-power pulsed magnetron discharge. *IEEE Transactions on Plasma Science 33*(2), 346–347.

Bohlmark, J., M. Lattemann, J. T. Gudmundsson, A. P. Ehiasarian, Y. A. Gonzalvo, N. Brenning, and U. Helmersson (2006). The ion energy distributions and ion flux composition from a high power impulse magnetron sputtering discharge. *Thin Solid Films 515*(5), 1522–1526.

Brenning, N., J. T. Gudmundsson, D. Lundin, T. Minea, M. A. Raadu, and U. Helmersson (2016). The role of ohmic heating in dc magnetron sputtering. *Plasma Sources Science and Technology 25*(6), 065024.

Brenning, N., J. T. Gudmundsson, M. A. Raadu, T. J. Petty, T. Minea, and D. Lundin (2017). A unified treatment of self-sputtering, process gas recycling, and runaway for high power impulse sputtering magnetrons. *Plasma Sources Science and Technology 26*(12), 125003.

Depla, D., S. Mahieu, and R. De Gryse (2009). Magnetron sputter deposition: Linking discharge voltage with target properties. *Thin Solid Films 517*(9), 2825–2839.

Fetisov, I. K., G. V. Khodachenko, and D. V. Mozgrin (1991). Quasy-stationary high current forms of low pressure discharge in magnetic field. In V. Palleschi and M. Vaselli (Eds.), *Proceedings of the XX international conference on phenomena in ionized gases : Il Ciocco (Barga, Italy) 8th - 12th July 1991*, pp. 474–475.

References

Gudmundsson, J. T. (2008). Ionized physical vapor deposition (IPVD): Magnetron sputtering discharges. *Journal of Physics: Conference Series 100*, 082002.

Gudmundsson, J. T. (2016). On reactive high power impulse magnetron sputtering. *Plasma Physics and Controlled Fusion 58*(1), 014002.

Gudmundsson, J. T., J. Alami, and U. Helmersson (2002). Spatial and temporal behavior of the plasma parameters in a pulsed magnetron discharge. *Surface and Coatings Technology 161*(2-3), 249–256.

Gudmundsson, J. T., N. Brenning, D. Lundin, and U. Helmersson (2012). The high power impulse magnetron sputtering discharge. *Journal of Vacuum Science and Technology A 30*(3), 030801.

Gudmundsson, J. T., D. Lundin, N. Brenning, M. A. Raadu, C. Huo, and T. M. Minea (2016). An ionization region model of the reactive Ar/O_2 high power impulse magnetron sputtering discharge. *Plasma Sources Science and Technology 25*(6), 065004.

Hajihoseini, H. and J. T. Gudmundsson (2017). Vanadium and vanadium nitride thin films grown by high power impulse magnetron sputtering. *Journal of Physics D: Applied Physics 50*(50), 505302.

Hubička, Z., J. T. Gudmundsson, P. Larsson, and D. Lundin (2020). Hardware and power management for high power impulse magnetron sputtering. In D. Lundin, J. T. Gudmundsson, and T. Minea (Eds.), *High Power Impulse Mangetron Sputtering: Fundamentals, Technologies, Challenges and Applications*, pp. 49–80. Amsterdam, The Netherlands: Elsevier.

Huo, C., D. Lundin, J. T. Gudmundsson, M. A. Raadu, J. W. Bradley, and N. Brenning (2017). Particle-balance models for pulsed sputtering magnetrons. *Journal of Physics D: Applied Physics 50*(35), 354003.

Huo, C., D. Lundin, M. A. Raadu, A. Anders, J. T. Gudmundsson, and N. Brenning (2013). On sheath energization and ohmic heating in sputtering magnetrons. *Plasma Sources Science and Technology 22*(4), 045005.

Huo, C., D. Lundin, M. A. Raadu, A. Anders, J. T. Gudmundsson, and N. Brenning (2014). On the road to self-sputtering in high power impulse magnetron sputtering: particle balance and discharge characteristics. *Plasma Sources Science and Technology 23*(2), 025017.

References

Kateb, M., H. Hajihoseini, J. T. Gudmundsson, and S. Ingvarsson (2019). Role of ionization fraction on the surface roughness, density, and interface mixing of the films deposited by thermal evaporation, dc magnetron sputtering, and HiPIMS: An atomistic simulation. *Journal of Vacuum Science and Technology A 37*(3), 031306.

Kouznetsov, V. (2001). Method and apparatus for magnetically enhanced sputtering. U.S Patent no. 6,296,742 B2 (October 2, 2001).

Kouznetsov, V., K. Macák, J. M. Schneider, U. Helmersson, and I. Petrov (1999). A novel pulsed magnetron sputter technique utilizing very high target power densities. *Surface and Coatings Technology 122*(2-3), 290–293.

Lundin, D., A. Hecimovic, T. Minea, A. Anders, N. Brenning, and J. T. Gudmundsson (2020). Physics of high power impulse magnetron sputtering discharges. In D. Lundin, J. T. Gudmundsson, and T. Minea (Eds.), *High Power Impulse Mangetron Sputtering: Fundamentals, Technologies, Challenges and Applications*, pp. 265–332. Amsterdam, The Netherlands: Elsevier.

Magnus, F., O. B. Sveinsson, S. Olafsson, and J. T. Gudmundsson (2011). Current-voltage-time characteristics of the reactive Ar/N_2 high power impulse magnetron sputtering discharge. *Journal of Applied Physics 110*(8), 083306.

Magnus, F., T. K. Tryggvason, S. Olafsson, and J. T. Gudmundsson (2012). Current-voltage-time characteristics of the reactive Ar/O_2 high power impulse magnetron sputtering discharge. *Journal of Vacuum Science and Technology A 30*(5), 050601.

Magnus, F., A. S. Ingason, S. Olafsson, and J. T. Gudmundsson (2012). Nucleation and resistivity of ultrathin TiN films grown by high power impulse magnetron sputtering. *IEEE Electron Device Letters 33*(7), 1045 – 1047.

Mozgrin, D. V. (1994). *High-current low-pressure quasi-stationary discharge in a magnetic field: Experimental research*. Ph. D. thesis, Moscow Engineering Physics Institute (MEPhI), (in Russian).

Panjan, M. and A. Anders (2017). Plasma potential of a moving ionization zone in DC magnetron sputtering. *Journal of Applied Physics 121*(6), 063302.

Raadu, M. A., I. Axnäs, J. T. Gudmundsson, C. Huo, and N. Brenning (2011). An ionization region model for high power impulse magnetron sputtering discharges. *Plasma Sources Science and Technology 20*(6), 065007.

Samuelsson, M., D. Lundin, J. Jensen, M. A. Raadu, J. T. Gudmundsson, and U. Helmersson (2010). On the film density using high power impulse magnetron sputtering. *Surface and Coatings Technology 202*(2), 591–596.

Thornton, J. A. (1978). Magnetron sputtering: basic physics and application to cylindrical magnetrons. *Journal of Vacuum Science and Technology 15*(2), 171–177.